Wettability: Fundamentals and Surface Forces

G.J. Hirasaki, SPE, Shell Development Co.

Summary. The wetting of mineral surfaces by water and oil is described by models of surface forces that become important when two surfaces approach each other. Force components are electrostatic, van der Waals, and structural. The electrostatic force depends on brine pH and salinity, crude oil composition, and the mineral. The surface forces are expressed as a disjoining pressure isotherm, and its integral is the specific interaction potential isotherm. The specific interaction potential isotherm can be used to determine the stable and metastable film-thickness profiles at the three-phase contact region for a given capillary pressure and/or curvature of the substrate. This profile gives the contact angle.

Introduction

Wettability has been recognized as an important factor in remaining oil saturation and in capillary pressure and relative permeability curves.[1,2] This work describes some of the physics of the contact angle between mineral surfaces, water, and oil. Description of a particular system requires a chemical description of the mineral, brine, and oil. The wettability of a rock/brine/oil system cannot be described by a single contact angle because it is the multitude of contact angles at the various three-phase contact regions in the pore spaces that determines system wettability. A complete wettability description requires a morphological description of the pore space with the contact angles as a boundary condition for the fluid distribution. Regardless of the morphology, however, the wettability depends on the contact angles. This work focuses on the intermolecular surface forces that affect wettability. A tremendous amount of research on this subject exists outside the petroleum industry that can be applied to petroleum reservoirs. The state of the art is reviewed in Refs. 3 through 6. Mohanty[7] applied these concepts to the fluid distribution in petroleum reservoirs, and Hirasaki[8] elaborated on the development of Mohanty's applied theory.

The intermolecular surface force approach originated with Derjaguin and Landau's and Verwey and Overbeek's (DLVO) theory of colloidal stability.[3-5] This theory describes the stability and flocculation of lyophobic (solvent-fearing) colloids, considering electrostatic and van der Waals interactions. This approach has been used [9-12] to describe the stability of the wetting-water film. The present work goes beyond the stability of the wetting-water film to examine the value of the contact angle when the wetting film collapses. To describe the contact angle, it is necessary to consider other surface forces, collectively called structural forces. Description of wettability in petroleum reservoirs requires the inclusion of capillary pressure and the curvature of the pore walls.

This paper reviews the extensive literature on the physics and chemistry of wettability that resides outside the petroleum literature. The new information describes how fundamental surface forces affect wettability in petroleum reservoirs and the magnitude of advancing and receding contact angles for oil/water/mineral systems in terms of surface forces. This work is intended to provide a guide for researchers investigating wettability mechanisms.

Thermodynamics of Wettability

The thermodynamics of wettability[4-6,8,13,14] requires a description of the region where three phases come together at the contact line, as shown in **Fig. 1**. When a pair of interfaces approach each other at a three-phase contact line, the interfaces interact with each other, and the distance separating the interface affects the system energy. Thus, this distance—called thickness—is a thermodynamic variable. The change in energy per unit area with change in distance as the pair of interfaces is brought from a large separation to a finite thickness is expressed as a force per unit area or disjoining pressure, Π. The disjoining pressure is the force that tends to disjoin or separate the two interfaces. A negative disjoining pressure attracts the two interfaces.

The conditions for equilibrium of a system with a pair of interfaces are equality of temperature and chemical potentials between the phases and the augmented Young-Laplace equation,

$$p^{\alpha}-p^{\gamma}=\Pi+2H^{\alpha\gamma}\sigma^{\alpha\gamma}, \quad \ldots\ldots\ldots\ldots\ldots\ldots\ldots\ldots (1)$$

where $H^{\alpha\gamma}$ = mean curvature, $\sigma^{\alpha\gamma}$ = interfacial tension (IFT), and $p^{\alpha}-p^{\gamma}$ = Laplace pressure or capillary pressure, P_c. In the meniscus region where the separation of the interfaces is large, $\Pi=0$ and Eq. 1 reduces to the usual Young-Laplace equation. If one of the bulk phases is a flat solid, the mean curvature of the fluid/fluid interface is zero where the interfaces are parallel. Here, $P_c=\Pi$.

A free-energy function is needed to determine the configuration of the equilibrium interface in the three-phase contact region. The thermodynamic potential (or free energy) that is a minimum for processes at fixed temperature, volume, and chemical and gravitational potentials is the grand canonical potential, Ω. This potential has been called the "interaction potential" in the DLVO theory of colloidal science (defined with zero capillary pressure such that it is zero at infinite separation). Ω, however, differs from the DLVO interaction potential because the disjoining pressure at equilibrium can be nonzero if the capillary pressure is nonzero. Here, Ω describes the energy of interaction of two phases separated by a third phase as a function of the separation distance. The departure of the film thickness from the equilibrium thickness results in an increase of this potential from the minimum value, described by

$$\Delta\omega=\int_{h}^{h_{eq}}[\Pi(h')-\Pi_{eq}]dh', \quad \ldots\ldots\ldots\ldots\ldots\ldots\ldots\ldots (2)$$

where ω = potential per unit area (or specific interaction potential) and Π_{eq} = value of equilibrium disjoining pressure that satisfies Eq. 1 and equals the capillary pressure if the solid substrate is flat. **Fig. 2** illustrates the relationship between the disjoining pressure and this specific interaction potential. The isotherm equals Π_{eq} at three thicknesses, h_1, h_2, and h_{eq}. h_1 is an unstable equilibrium point. Suppose that the film is at the metastable equilibrium thickness, h_{eq}. The potential energy change from h_{eq} to h_1 is shown by the shaded areas. If the negative area is greater than the positive area, then h_2 will have a lower value of specific interaction potential than h_{eq} and h_{eq} is metastable. The energy barrier between the two local equilibria is shown by the peak in the potential at h_1 and by the positive area in the upper portion of Fig. 2. The two thicknesses can coexist if the potential values are equal.

The magnitude of the minimum of the specific interaction potential (relative to infinite separation) determines the value of the macroscopic contact angle, as will be shown later. When $P_c=0$, the negative value of specific interaction potential at the minimum is the work required to separate the bulk phases. It can be interpreted as the work of adhesion in the presence of a third phase (usually vacuum or vapor) or the spreading coefficient. If this work is zero or less, $\theta=0$. If this work equals the IFT, then $\theta=90°$.

Contact Angle and Film Stability

The contact angle[4-8,15] is the angle of the macroscopic meniscus when extrapolated to zero thickness (**Fig. 3**). Young's equation of

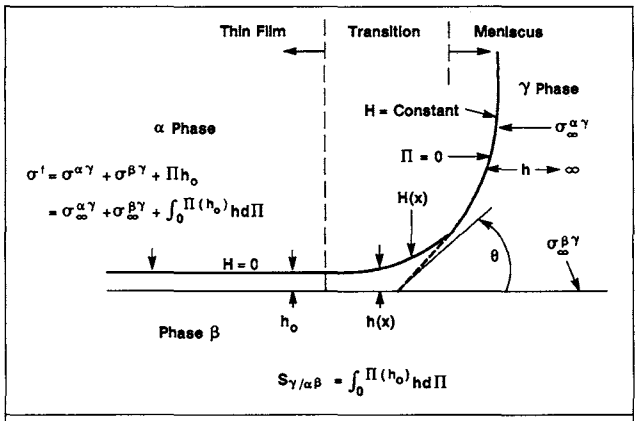

Fig. 1—Contact region between two fluids and a solid. T, μ_c, and Φ_g are constant.

the contact angle, expressed as a function of the surface energies or IFT's, is a statement of mechanical equilibrium. The difference of surface energies in Young's equation equals the difference in the specific interaction potential between the equilibrium thickness and infinite separation (when $P_c=0$).

An alternative determination of the contact angle is to integrate the augmented Young-Laplace equation (Eq. 1).[7,8,13-15] Integration of the mean curvature term gives the cosine of the angle of inclination of the microscopic meniscus from the flat solid. One minus the cosine of the angle equals the specific interaction potential divided by the fluid/fluid IFT (**Fig. 4**). Angle increases or decreases identify the concave and convex regions of the microscopic meniscus. Along the macroscopic meniscus, where $\Pi=0$, $1-\cos\alpha$ is a straight line with a slope equal to the capillary pressure divided by the IFT. This straight-line region can be extrapolated to zero thickness to determine the contact angle.

$$1-\cos\theta=\left[-\int_{h_o}^{\infty}\Pi dh-h_o\Pi(h_o)\right]/\sigma=-(S_{\gamma/\alpha\beta})/\sigma. \quad \ldots\ldots (3)$$

If the extrapolated value of $1-\cos\alpha$ is negative, then a nonzero contact angle does not exist because the macroscopic meniscus becomes tangent to the solid. If the extrapolated value is positive, then a nonzero contact angle exists. If the extrapolated value equals 1.0, then $\theta=90°$. A thin film of the original film phase, however, may still exist—e.g., water of hydration on an oil-wet mineral surface.

The system in Fig. 4 has two different locally stable film thicknesses, h_1 and h_2. h_1 has a finite contact angle, and h_2 does not. In Fig. 4, the thinner film has lower energy and thus is more stable. If the system is formed by thinning from a large separation, however, the film may thin only to the metastable film at h_2 be-

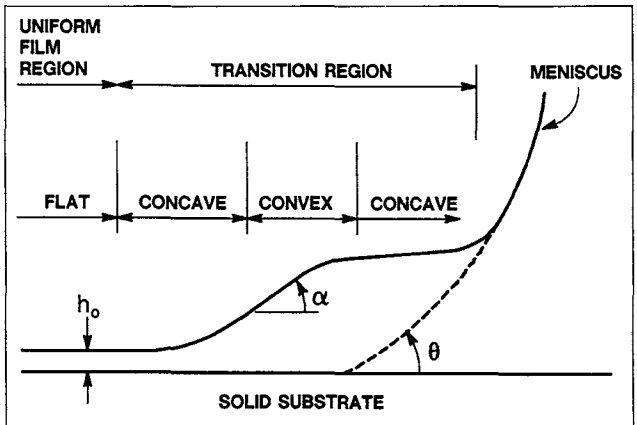

Fig. 3—Profile of film/meniscus transition zone.

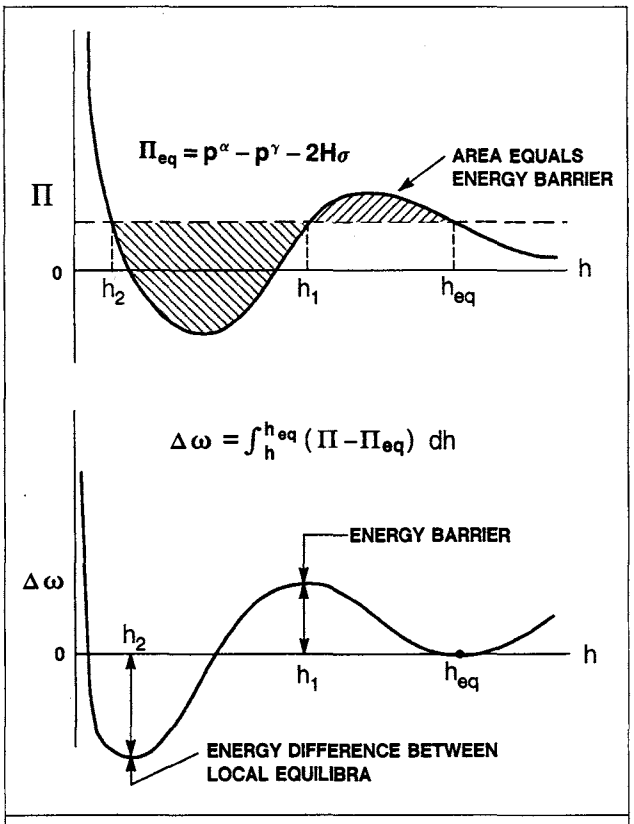

Fig. 2—Isotherms of disjoining pressure and specific interaction potential.

cause of the energy barrier separating the local equilibrium states. In this case, $\theta=0$. On the other hand, if the film is formed by adsorption from zero thickness, then it will not increase beyond h_1, and the system will have a finite contact angle. The effect of metastable film states results in contact angle hysteresis. The contact angle at a given capillary pressure depends on the history of the film's arrival at equilibrium.

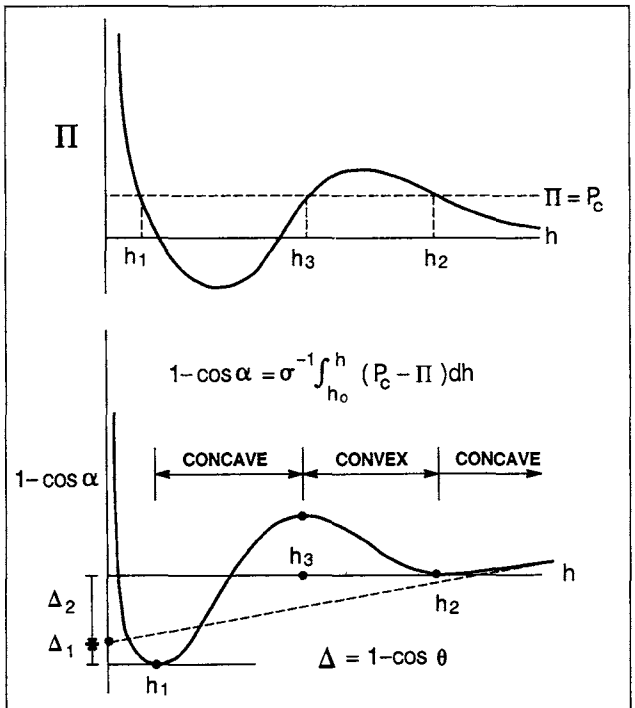

Fig. 4—Disjoining pressure and angle of inclination.

As the capillary pressure increases for the system in Fig. 4, h_3 approaches h_2, and the energy barrier separating the two metastable states decreases. Above some critical capillary pressure, the metastable film with zero contact angle will no longer exist.

Disjoining Pressure Components

Disjoining pressure results from intermolecular or interionic forces. The contributions are identified as van der Waals, electrostatic, and structural or solvation forces. The first two contributions were introduced about 1940 to explain colloid stability. The theory has been called the DLVO theory[3-5] after Derjaguin and Landau of the Soviet Union and Verwey and Overbeek of the Netherlands.

van der Waals Interactions. The Hamaker constant (coefficient of the dependence of energy on distance) of thin films can be calculated from the refractive index, dielectric constant, and absorption frequencies of the materials. The results show that the Hamaker constant of mineral/water/oil systems strongly depends on the materials.

van der Waals forces exist between all matter, and thus, are an important component of the surface forces in thin films. A modern approach to quantification of the van der Waals surface energy is the Lifshitz theory,[16] which is based on quantum field theory. For quantification, this approach requires the dielectric properties of the media, such as the zero-frequency dielectric constant, the refractive index, and absorption frequencies. An approximation that uses only these parameters is used here to calculate the Hamaker constant for mineral/water/oil systems.

The traditional approach of van der Waals interactions is based on the Hamaker theory, which assumes that the interactions are pair-wise additive and independent of the intervening media and that the interaction between two different media is the geometric mean of the interaction of each medium with itself. The modern approach shows that these assumptions are good if the only interactions are the London dispersion forces (induced dipole/induced dipole) but are not accurate when the Keesom and Debye contributions of polar materials are significant.[3-5]

Interaction for Plane-Parallel Film. Israelachvili[3] reviews the approximations that lead to the following expression for the Hamaker constant of Materials 1 and 2 separated by Material 3:

$$A = A_{\nu=0} + A_{\nu>0}, \quad \ldots\ldots\ldots\ldots\ldots\ldots\ldots\ldots\ldots\ldots\ldots\ldots (4a)$$

where $A_{\nu=0} = \frac{3}{4}kT[(\epsilon_1-\epsilon_3)/(\epsilon_1+\epsilon_3)][(\epsilon_2-\epsilon_3)/(\epsilon_2+\epsilon_3)] \quad \ldots (4b)$

and $A_{\nu>0} \approx$

$$\frac{3P\nu_e}{8\sqrt{2}} \frac{(n_1^2-n_3^2)(n_2^2-n_3^2)}{(n_1^2+n_3^2)^{1/2}(n_2^2+n_3^2)^{1/2}[(n_1^2+n_3^2)^{1/2}+(n_2^2+n_3^2)^{1/2}]}. \quad \ldots\ldots\ldots\ldots\ldots\ldots\ldots\ldots\ldots\ldots\ldots\ldots (4c)$$

The material parameters are as follows: the zero-frequency dielectric constant, ϵ_1; the refractive index in the visible part of the spectrum extrapolated to zero frequency, n_i; and the electronic absorption or ionization frequency, ν_e, which is assumed to be the same for each material. This frequency is similar for water, quartz, and alkanes but is smaller for aromatic compounds. T is the absolute temperature, and k and P are Boltzmann's and Plank's constants, respectively. The above relation does not include the effect of retardation resulting from the finite speed of electromagnetic interactions, but this effect only decreases the Hamaker constant for film thicknesses greater than about 5 nm. The interaction energy is calculated from the Hamaker constant and the film thickness:

$$\omega(h) = -(A/12\pi)h^{-2}. \quad \ldots\ldots\ldots\ldots\ldots\ldots\ldots\ldots\ldots\ldots\ldots\ldots (5)$$

The Hamaker constant in the form given by Eq. 5 consist of two terms: (1) a zero-frequency, dielectric-constant-dependent term proportional to the temperature, and (2) a frequency-and-refractive-index-dependent term that does not have an explicit dependence on temperature. The first term is an entropic term resulting from the Keesom and Debye forces of polar molecules. The second term results from London dispersion forces. The van der Waals contribution to the disjoining pressure is negative or attractive when the Hamaker constant is positive and is positive or repulsive when the Hamaker constant is negative. Each term in Eq. 4 is negative if the value of the material parameter of the film material is between those of the bulk phases; otherwise, it is positive.

The traditional approach[17-19] to calculating the Hamaker constant of a film assumed that the interactions are pair-wise additive and that the interaction between two different media is the geometric mean of the interactions of each medium with itself. The expression for the Hamaker constant of a film of Material 3 between Materials 1 and 2 with these assumptions is

$$A_{132} = (A_{11}^{1/2} - A_{33}^{1/2})(A_{22}^{1/2} - A_{33}^{1/2}). \quad \ldots\ldots\ldots\ldots\ldots\ldots\ldots\ldots\ldots\ldots\ldots\ldots (6)$$

Eq. 6 shows that if the Hamaker constant of the film material has a value between those of the bulk phases, then the composite Hamaker constant of the film is negative; otherwise, it is positive. This relation between the material parameters is similar to each term of the expressions in Eq. 4.

Interaction With Adsorbed Layer on Substrate. The preceding discussed a film of Material 3 between bulk phases of Materials 1 and 2. The van der Waals interactions can also be described when the bulk phase has one or more adsorbed layers. Parsegian and Ninham[20] described how to include adsorbed layers in the Lifshitz theory. Vold[21] and Vincent[22] included the effect of adsorbed layers, assuming pair-wise additivity and geometric mean interactions between dissimilar media. The latter approach will be used here. Suppose that the bulk phase of Material 1 has an adsorbed layer of Material 4 of thickness δ. The film phase is of Material 3 of thickness h, and the other bulk phase is of Material 2. The van der Waals interaction potential is derived from summation of pair-wise interactions (including addition and subtraction of terms so that the remaining terms are interactions of semi-infinite bodies across a gap) and the assumption of geometric mean interaction between dissimilar media. The interaction potential for this case is

$$\omega(h) = \frac{(A_{11}^{1/2} - A_{44}^{1/2})(A_{22}^{1/2} - A_{33}^{1/2})}{12\pi(\delta+h)^2} + \frac{(A_{44}^{1/2} - A_{33}^{1/2})(A_{22}^{1/2} - A_{33}^{1/2})}{12\pi h^2} \quad \ldots\ldots\ldots\ldots\ldots\ldots\ldots\ldots\ldots\ldots\ldots\ldots (7)$$

When δ is small compared with h, the interaction approaches the case in the absence of an adsorbed layer—i.e., film of Material 3 between bulk phases of Materials 1 and 2. When δ is large compared with h, the interaction approaches that for a film of Material 3 between bulk phases of Materials 4 and 2. Thus, as h changes from small to large compared with δ, the interaction changes from one with Material 4 as the bulk phase to one with Material 1 as the bulk phase. This can change the sign of the interactions.

Electrostatic Interactions. A model of the electrical double-layer interaction as two surfaces approach each other in an aqueous medium is discussed. The interaction can be repulsive, attractive, or a combination. The model is used to calculate the necessary condition for the stability of a thick, wetting-water film.

When two charged bodies approach each other in a vacuum, the interactions are governed by Coulomb's law. When the intervening medium is water, the interactions are complicated by the presence of the electrolyte ions. The electrical field near a charged surface decays approximately exponentially with a decay length called the Debye length that is inversely proportional to the square root of the electrolyte concentration. This electrical field, or electrical double layer, extends about 1.0 nm in 0.1 M NaCl. When two charged surfaces approach each other in water, the overlap of the double layers will cause a change in the system energy. The energy differential with respect to the water-film thickness is a force or, expressed per unit area, the electrical contribution to the disjoining pressure. How the energy and disjoining pressure change as a function of the film thickness and the system parameters is discussed below.

Model for Double-Layer Interactions. The interaction of two identical double layers is the foundation of the DLVO theory for colloidal stability. The interaction of dissimilar double layers is approximated for low potentials and smeared charges by analytical

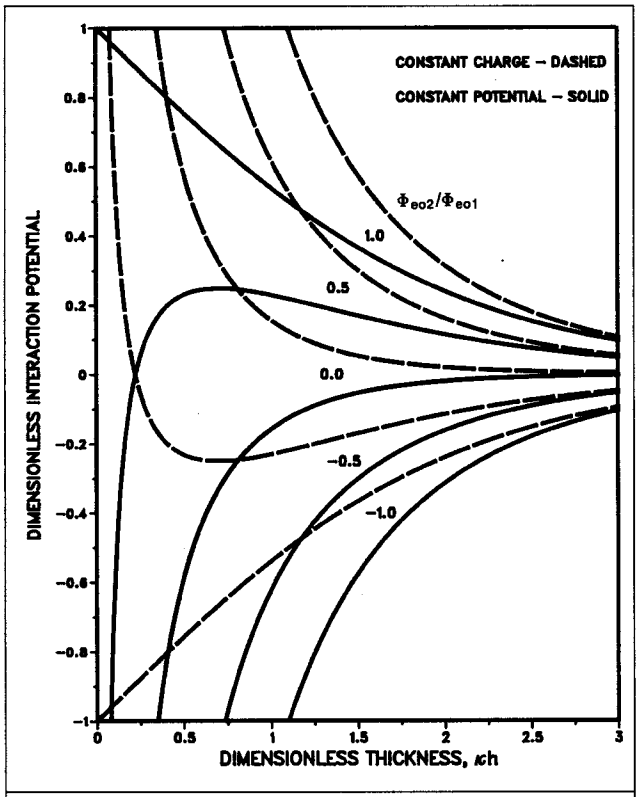

Fig. 5—Electrostatic specific interaction potentials for constant charge and potential models.

solutions of Hogg *et al.*[23] for the constant surface electrical-potential case and by Usui[24] for the constant surface electrical-charge case. These limiting cases of constant potential or charge as the surfaces approach each other bracket the case of constant electrochemical potential, or charge regulation,[25] in which both the potential and the charge change as the surfaces approach each other. The electrostatic specific (unit-area) interaction potential for these limiting cases can be expressed by the following equation.

$$\omega_D = 1/2[\pm(1+F_{\Phi_e}^2)(\coth h_D - 1) + 2F_{\Phi_e} \operatorname{cosech} h_D]. \quad \ldots\ldots(8)$$

The dimensionless interaction potential is

$$\omega_D = \omega/\epsilon_o \epsilon \kappa \Phi_{eo1}^2, \quad \ldots\ldots(9)$$

where Φ_{eo1} is the surface electrical potential of Surface 1 at infinite separation. The ratio of the potentials at infinite separation is

$$F_{\Phi_e} = \Phi_{eo2}/\Phi_{eo1}. \quad \ldots\ldots(10)$$

The dimensionless distance is

$$h_D = \kappa h. \quad \ldots\ldots(11)$$

The reciprocal of the Debye length is

$$\kappa = (e^2 \Sigma C_i^o z_i^2/\epsilon_o \epsilon kT)^{1/2}. \quad \ldots\ldots(12)$$

The plus sign in Eq. 8 applies for a constant surface charge, and the minus sign applies for a constant surface potential.

The interaction potentials for the constant-charge and constant-potential cases are shown in **Fig. 5** for five different potential ratios. When both potentials have the same sign, the interaction potential with constant charge is always positive, but the interaction potential with constant potential becomes negative at some small thickness unless the two potentials are the same. This attraction of two surfaces of constant potential of the same sign but different magnitudes results from a charge reversal on the surface with the lower potential when the electrical field is dominated by that of the surface with the higher potential.

Eq. 8 and Fig. 5 show that if the constant potential and constant charge curves are mirror images of each other, then the sign of F_{Φ_e} is reversed.[18] If the potential curves have opposite signs, the constant-potential case will always be attractive, but the constant-charge case will become repulsive at small thicknesses unless the magnitude of the surface charge is identical. The results for charge regulation[25] will be intermediate between these two cases.

TABLE 1—ISOELECTRIC POINT AND POINT OF ZERO CHARGE OF MINERALS[26–29]

Mineral	pH
Quartz	2 to 3
Calcite	8 to 9.5
Alumina	7 to 9
Brucite	12
Hematite	6 to 9

The effect of the electrolyte concentration and valence can be examined by the dependence of the dimensionless thickness on κ, which is proportional to the square root of the electrolyte concentration. The dimensional distance over which the interactions become important is inversely proportional to the square root of the electrolyte concentration. Also, for a given charge density, the surface electrical potential is approximately inversely proportional to the square root of the electrolyte concentration (for small potentials).

Measurement of Surface Electrical Potentials. The electrical potential at the water/oil and water/mineral interfaces can be estimated from the measurement of the zeta potential with electrokinetic methods.[16,26-28] An example of such measurements is described by Buckley *et al.*,[12] who show the zeta potential of these surfaces to be a function of pH and salinity by using a site-dissociation model to represent acid and base sites on the surfaces. As a function of the pH, the surface has a positive zeta potential below and a negative zeta potential above the isoelectric pH.

Quartz has negative zeta potentials (at least above a pH of 2), but other minerals have different isoelectric points and have specific ion effects. **Table 1** lists the isoelectric points of some minerals.

Clays are not included in Table 1 because they have different charges on different surfaces.[30] The charge on the faces results mainly from isomorphous substitution of elements in the crystal lattice and is negative. The edges can be positive, similar to alumina, brucite, or hematite.

Structural or Solvation Interactions in Thin Films. The models used to describe the van der Waals and electrostatic interactions treat the bulk and film phases as if they are a continuum with uniform properties up to the interfaces. These models are adequate only as long as the film thickness is large compared with the size of the molecules or any other inhomogeneity on the surface or in the film. For example, the van der Waals interaction potential for a material separated by a vacuum goes to infinity if the separation distance goes to zero. At contact, this potential should be equal to twice the surface energy or surface tension. We know that the center of mass of two molecules cannot coincide, and a large repulsion sets in when the molecular diameter is approached. Also, the molecules on opposite sides of the contact region can arrange to pack efficiently. Thus, to calculate the surface energy or surface tension from the van der Waals model, the interaction potential must be calculated at some cutoff distance that is less than the molecular diameter; e.g., a distance of 0.165 nm has been used for hydrocarbons.[3] If the two bulk phases are separated by a film of another material, the effect of molecular packing becomes important when the film thickness approaches the molecular distances. Experiments that used large molecules between mica sheets show the force to oscillate with a period equal to the molecular diameter.[3,29]

Although the van der Waals and electrostatic models included some of the polar properties of water, through the Debye and Keesom terms and the dielectric constant, these models do not include the effect of hydrogen bonding and specific ion/water interactions. These are called solvation or hydration effects or structural forces because they are a result of the intermolecular structure of the solvent or water.[31] The result can be either a hydrophilic (water-loving) effect for a surface such as clean quartz or mica or a hydrophobic (water-hating) effect for a surface with an organic coat-

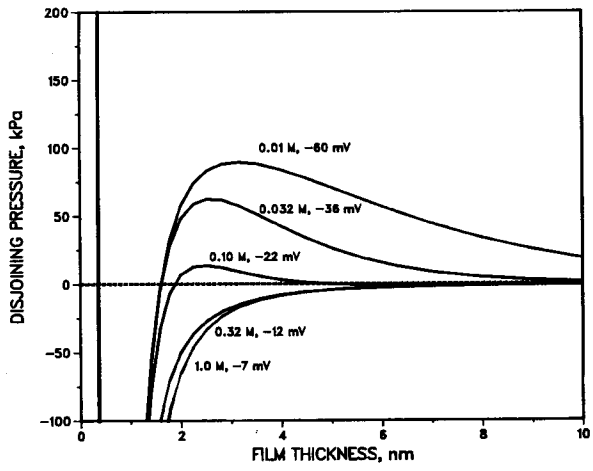

Fig. 6—Disjoining pressure isotherms for different electrolyte concentrations, 0.1 ion/nm^2; $A = 1 \times 10^{-20}$ J.

ing. Measurements with mica surfaces have shown these forces to be described as a sum of two exponential decay terms.[3] At very close separations, an oscillating component is observed.[3] These forces on mica are a function of pH and electrolyte composition.[3] Adsorption isotherms of water on silica show that these forces are greatly diminished as the temperature is raised to 65°C,[4-6] as may be expected for hydrogen-bonding effects. Other measurements demonstrate that the water near silica and clay surfaces is different from bulk water.[4-6] Water in submicrometer silica capillaries has a viscosity as much as 40% greater than that of bulk water, but this increase disappears at 70°C. Nuclear magnetic resonance measurements of this boundary layer have reported thicknesses to 10 nm. The static dielectric constant of water in Na montmorillonite and silica gel is significantly reduced from bulk values. Infrared spectra of water adsorbed on silica show a strengthening of intermolecular hydrogen bonds.

The assumption that the properties of the bulk and film phases are uniform up to the interface is certain to be in error for mixtures because components are adsorbed at the interfaces. In the case of electrolyte solutions, the effect of the ion concentration inhomogeneity is treated by the electrostatic interactions. Crude oils contain many components, and adsorption effects could result in the oil next to the interface having different dielectric properties from the bulk oil. For example, adsorption of asphaltene could result in a 1.0-nm layer having a refractive index near 1.6, while the bulk oil has a refractive index of about 1.4. If the thickness and properties of the adsorbed layer are known, then its effect could be included in the model for van der Waals forces with an adsorbed layer, as discussed earlier.

A gel layer will form on the surface of quartz when it is exposed to water at an elevated temperature for several days.[4,5] This gel layer shifts the adsorption isotherm of water from 2.5 to 3.0 nm. The van der Waals properties of this gel layer should be between those of quartz and water. If these properties are equal to those of water, then the layer thickness will correspond to the cutoff distance or limiting water-film thickness discussed later.

When the surface contains adsorbed polymers, the interfacial region is quite thick and the overlap of the adsorbed layers can contribute to additional forces called steric forces.[3]

The electrostatic models described earlier characterize the surfaces as having an electrical potential and surface charge density. These models treat the surface charges or ions as though they are uniformly distributed. The charge density on most surfaces is about one charge/nm^2 or less. If two surfaces containing opposite charges with at least one of the surfaces having mobile charges approach within 1 nm, the interaction may be much greater than if the charges were uniformly distributed.[4,5]

TABLE 2—MODEL PARAMETERS FOR BASE CASE

Hamaker constant, J	1×10^{-20}
Electrolyte concentration, *M*	0.01
Surface electrical potentials, mV	−60
Coefficient for structural force, kPa	1.5×10^{7}
Decay length for structural force, nm	0.05
Interfacial tension, mN/m	25

Stability of Wetting-Water Layer

A thick, wetting-water film will be (meta)stable if an adequate energy barrier exists between the thick, wetting film (with zero or small contact angle) and a thin water film (with a significant contact angle). In the case of zero capillary pressure and a flat surface, the condition of marginal stability is when the sum of the electrostatic and the van der Waals interaction potentials (structural forces are not significant in thick films) has only a local maximum (i.e., inflection point) in the thick-film region. This is equivalent to $\Pi = 0$ and $d\Pi/dh = 0$. This stability condition still allows the possibility of a small contact angle at a secondary minimum in the interaction potential curve. The DLVO stability condition for colloids differs from the stability condition for thin films. The stability condition for colloids is that the local maximum in the interaction potential is equal to or greater than zero. The energy barrier is measured with respect to zero, or the value at infinite separation, because the particles approach each other from large separations and the kinetic energy may pass it across the secondary minimum on its way to the local maximum. Usui[18] derived the conditions for colloidal stability in an unsymmetrical system using Eq. 8 for the electrical interaction potential. It is assumed that the maximum occurs at a large thickness, compared with the Debye thickness. This assumption simplifies Eq. 8 and gives a result independent of the assumption of whether the charge or potential is held constant. Usui's theory is modified for the condition of film stability with zero capillary pressure; i.e., the condition that the interaction potential has a local maximum between the thick, wetting film and the thin film, or equivalently, the disjoining pressure has a local maximum equal to or greater than zero. This results in the following expression for the minimum stable electrical potentials, which is the same as that of Usui except for the numerical coefficient:

$$\Phi_{eo1}\Phi_{eo2} = \exp(3)\kappa A/324\pi\epsilon_o\epsilon. \quad \ldots\ldots\ldots\ldots\ldots\ldots\ldots\ldots (13)$$

Fig. 6 shows the disjoining pressure isotherms for different electrolyte concentrations, assuming a charge density of 0.1 ion/nm^2 and a Hamaker constant of 1×10^{-20} J. The maximum of the disjoining pressure isotherm decreases with increasing electrolyte concentration and becomes negative slightly above 0.1 *M*. Above a 1.0-*M* concentration, the isotherm is dominated by the van der Waals forces except at small thicknesses, where the structural forces are important.

Buckley *et al.*[12] used adhesion tests to study the stability of thick, wetting-water films between glass and crude oil. Their stability condition was that the local maximum of the disjoining pressure had to be zero or a small positive value. This condition of zero disjoining pressure is given by Eq. 13.

Aronson *et al.*[32] investigated the stability of a water film between silica and an oil containing an oil-soluble cationic surfactant. For different combinations of surfactant concentrations and pH, the transition from stable to unstable water films occurred close to the transition from negative to positive zeta potential.

Example Model for Case Study

The effects of surface forces on wetting and the contact angle are illustrated with the parameters in **Table 2**. The value of the Hamaker constant represents the silica/water/oil system, discussed earlier, and is equal to the value used by Takamura[11] but greater than the range of 0.3 to 0.9×10^{-20} J used by Melrose.[9] The electrical potential of −60.0 mV represents the zeta potentials for silica and crude oils at neutral pH and a salinity of 0.02 *M*. The constant-surface-potential model for the electrostatic interactions was used throughout. The constant-charge model could have been used just

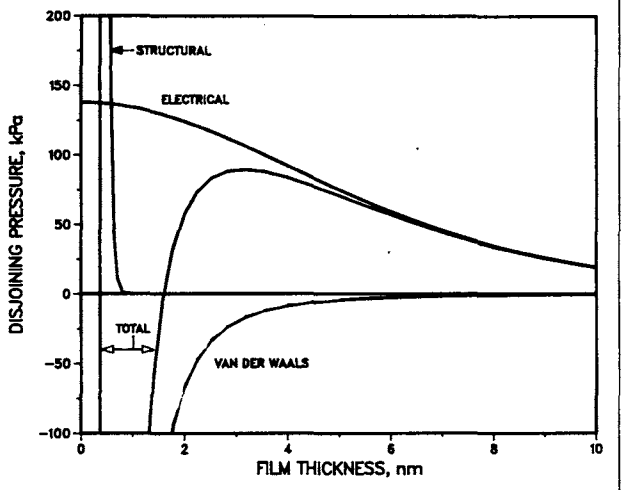

Fig. 7—Individual components of disjoining pressure isotherm for base case.

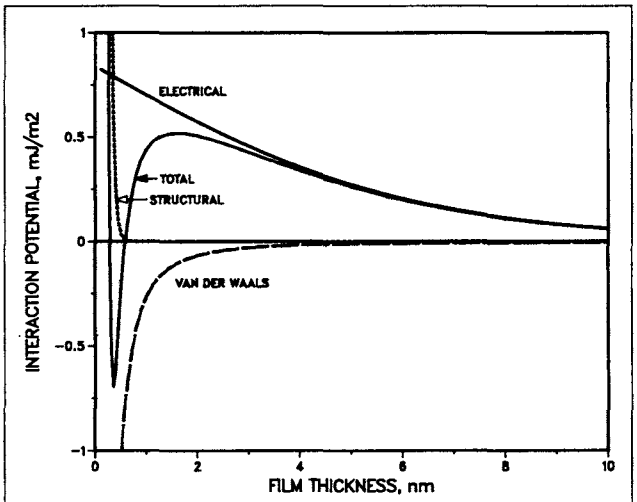

Fig. 8—Individual components of specific interaction potential isotherm for base case.

as well. Because the structural force for a silica/water/oil system is not known, a hypothetical, very steeply rising repulsion was used to represent the expected strong hydration binding of water to silica.

Fig. 7 shows the individual component and total disjoining pressure isotherms. **Fig. 8** shows the interaction potential isotherm for zero capillary pressure.

Capillary Pressure and Curvature for Wetting-Film Stability

Melrose[9] discussed the role of capillary pressure on the stability of a wetting-water film between silica and oil. The results here are generalized to include the effect of the solid curvature on stability. In the thermodynamics discussion, it was shown that for (meta)stability of a thicker film, the local maximum of the disjoining pressure isotherm must be greater than the capillary pressure minus the IFT times twice the mean curvature. This curvature is positive when the solid is concave and negative when the solid is convex. For example, a cylindrical pore that contains the hemispherical meniscus will have a capillary pressure and wall curvature such that the equilibrium value of the film's disjoining pressure equals one-half the capillary pressure. Where the pore surface is flat (zero curvature), the equilibrium disjoining pressure equals the capillary pressure, as Melrose[9] assumed. If the pore surface is irregular, the equilibrium disjoining pressure is less than the capillary pressure where it is concave and is greater than the capillary pressure where it is convex. Thus, instability of a film on a rough surface will first occur at a protrusion.

Fig. 9 shows the effect of the capillary pressure (the curvature of the solid is omitted for simplicity) on the stability of a thick wetting film. Consider cases of the equilibrium disjoining pressure equal to capillary pressures of 0, 20, 60, and 90 kPa. These cases each have three intersections with the isotherm, with the last intersection at 31, 9.8, 5.8, and 3.2 nm, respectively, the thickness of the thick wetting film. The 90-kPa case has the second and third intersections occurring about the same point near the peak of the isotherm. This capillary pressure is the critical value because a thick film cannot exist at a higher capillary pressure. The interaction potentials for these cases are shown in Fig. 9. The zeros of the potentials are chosen so that the isotherms coincide at small thick-

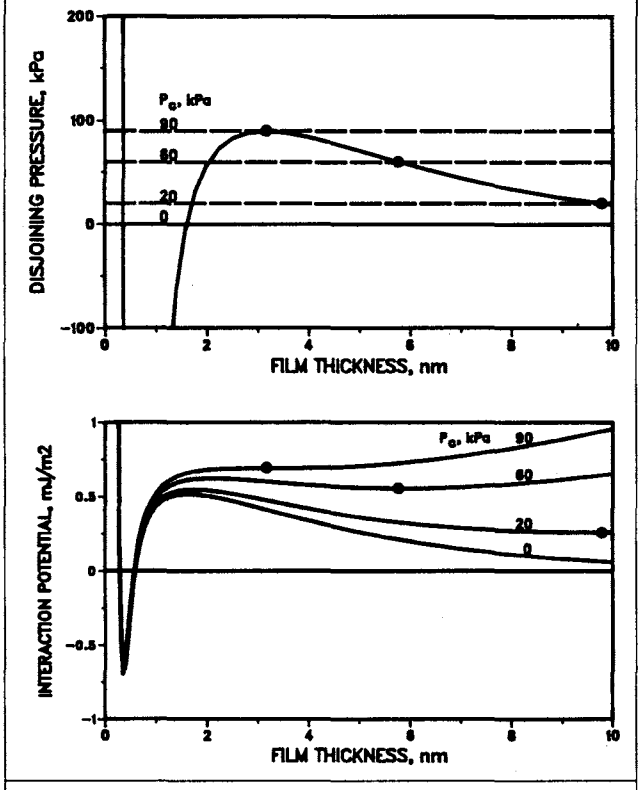

Fig. 9—Specific interaction potential isotherms for capillary pressures of 0, 20, 60, and 90 kPa.

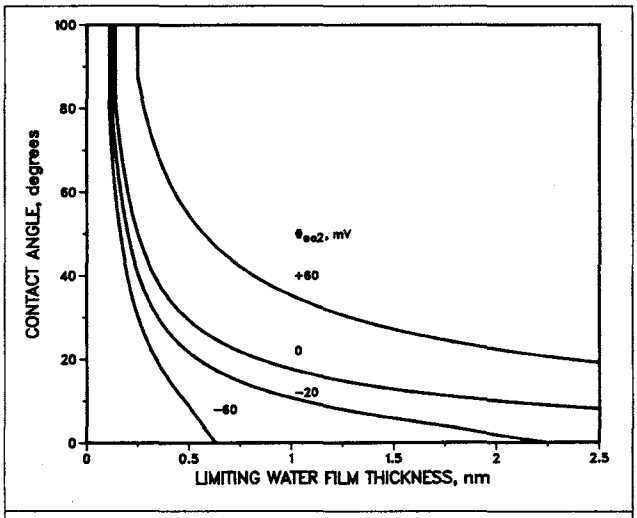

Fig. 10—Contact angles as function of limiting thickness of water film for different values of electrical potential on second surface, $C = 0.01$ *M*, and $\Phi_{eo1} = -60$ mV.

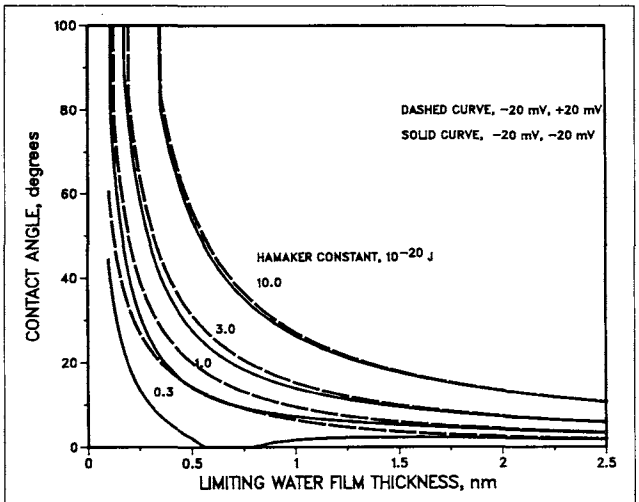

Fig. 11—Contact angles as function of limiting thickness of water film for different values of Hamaker constant and electrical potential on second surface, $C = 1.0$ *M*.

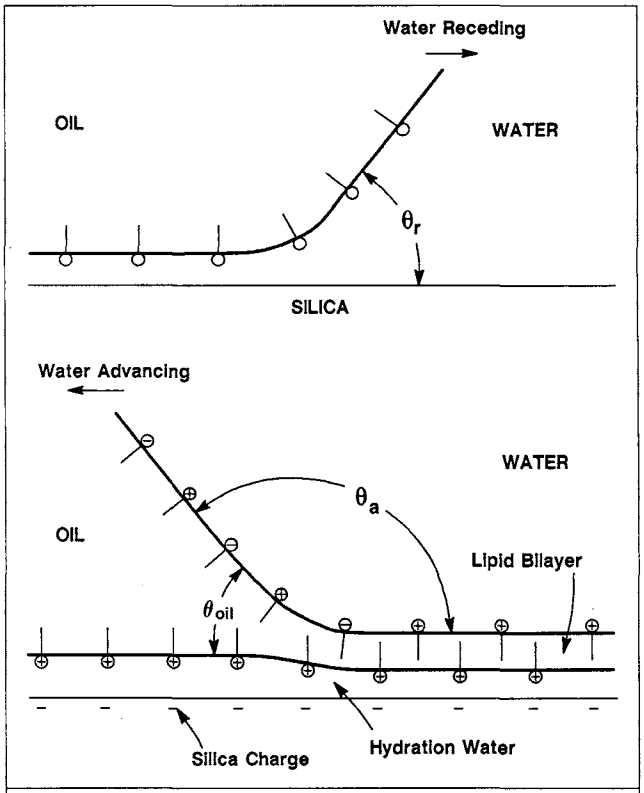

Fig. 12—Effect of surfactants on receding and advancing contact regions.

nesses. With the possible exception of the 90-kPa case, the interaction potential isotherms have a local (secondary) minimum at the thick wetting film. As the capillary pressure increases, the energy barrier decreases until it disappears at the 90-kPa (critical) case. If the system crosses the energy barriers to the primary minimum, the interaction potential equals −0.7 mN/m less than the extrapolated value (zero in this case). This thin film is 0.4 nm thick and has a 14° contact angle with the meniscus.

The wettability dependence on the capillary pressure has important implications for both reservoir environments and laboratory evaluations. It could result in water-wetting in a low-relief reservoir that overlies an oil/water contact and non-water-wetting in a high-relief reservoir with identical chemistry. When restoring wettability in laboratory cores, it may be necessary to bring the capillary pressure up to the reservoir conditions.

Effect of Surface Forces on Contact Angle

The contact angle will be calculated assuming that the water film has thinned to where the repulsive structural forces limit the thinning. The structural component of the disjoining pressure is modeled as an infinite repulsion below some limiting water-film thickness. The electrical potential of the second surface is varied, while that of the first surface is held fixed at −60 mV. It is assumed that the potentials remain constant and that the charge density changes as the surfaces approach each other. At small film thicknesses, the attractive van der Waals forces dominate the electrostatic forces, and the film will thin until limited by the structural forces. The results are illustrated in **Fig. 10** for an electrolyte concentration of 0.01 *M*. If the structural forces are not present (i.e., the solid surface is not hydrated), the film thins to zero thickness, where the interaction potential approaches negative infinity and the contact angle is >90°. As the limiting thickness resulting from the structural forces increases, the contact angle decreases because it limits or cuts off the interaction potential at this thickness. As a reference, one monolayer of water is about 0.3 nm thick. As the electrical potential of the second surface becomes increasingly different from that of the first surface, the contact angle increases because the electrical contribution to the interaction potential decreases and becomes negative. This example illustrates the importance of the presence of the hydration water on the mineral surface. If a dehydrated mineral surface is first contacted with oil, a large contact angle can result when it is subsequently contacted with water. Conversely, these results show that if the mineral has a layer of hydration water only one or two monolayers thick, the contact angle will be <90°.

Fig. 11 is an example with an electrolyte concentration of 1.0 *M*. Curves are shown for different values of the Hamaker constant and surface electrical potentials. The results at this high electrolyte concentration are not very sensitive to the electrical potential value (assuming smeared charges) except for the smallest value of the Hamaker constant. Again, the importance of the limiting water-layer thickness is illustrated. A discrete site model may show that electrostatic interactions are important at small separations when the surfaces have charges of opposite sign.

Oil Films and Contact Angle in Oil Phase

The preceding discussion of the contact angle when a thin water film exists between the mineral and oil applies during the accumulation of oil in a reservoir when water is the receding phase. During the waterflood stage, surface forces, such as those from natural crude oil surfactants, can result in an oil film remaining on the mineral surface, as shown in **Fig. 12**. Brown and Neustadter[33] observed contact angle hysteresis of an initial (water) receding value of 30° (in aqueous phase) and an advancing value of 180°. Assume that the structural forces retain a thin adsorbed layer of hydration water of thickness δ between the mineral surface and the oil film. Also assume that the structural forces of the steric interaction type resulting from the surfactants (such as asphaltenes) adsorbed on the two oil interfaces limit the thinning of the oil film. For example, Christenson and Israelachvili[34] measured a 3.5-nm hard-wall adsorbed asphaltene layer between mica surfaces. Any electrostatic interactions within the oil film are neglected. The contact angle in the oil phase is determined by the van der Waals interactions, with the cutoff distance determined by the steric interactions. The Hamaker constants used to calculate the van der Waals interaction from Eq. 7 are 6.5×10^{-20} J for quartz, 3.7×10^{-20} J for water, and 5.0×10^{-20} J for oil.[3]

Fig. 13 shows the disjoining pressure isotherms for an oil film between bulk water and a quartz surface with an adsorbed hydration water layer of thickness δ. If no hydration water is present, the disjoining pressure is positive or repulsive—i.e., oil wetting. The Hamaker constant of the oil is intermediate between quartz and water, which, from Eq. 7, means that this constant is negative. When the underlying water layer is thick, the disjoining pressure is negative, or attractive. Eq. 7 shows that when the water layer is very thick compared with the oil film, the Hamaker constant approaches that of an oil film between bulk water phases. For this case, the

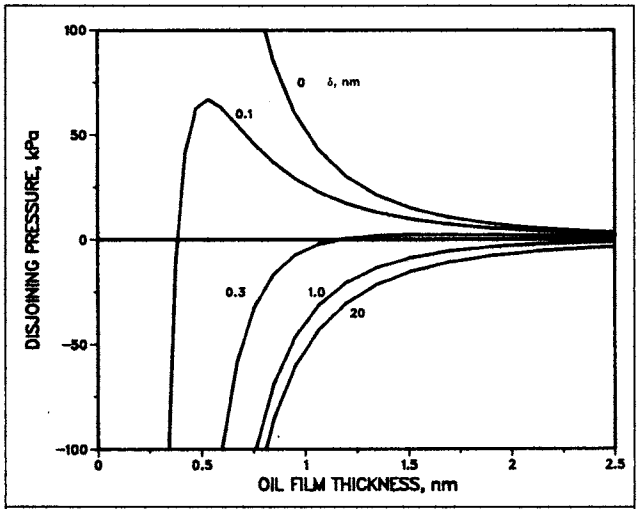

Fig. 13—Disjoining pressure isotherm for oil film over hydration water layer on silica substrate.

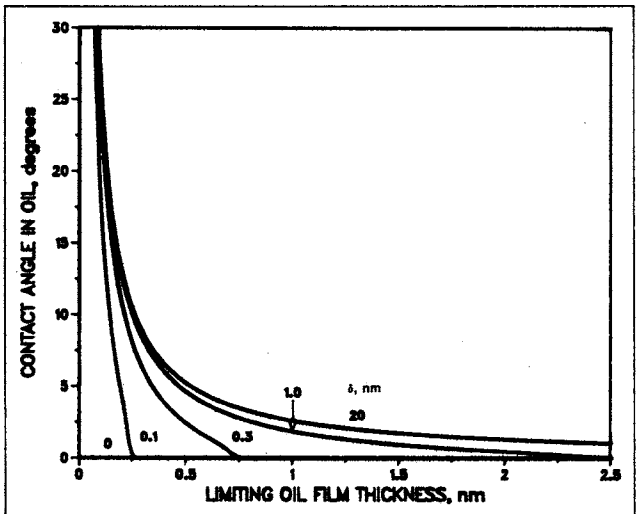

Fig. 14—Contact angles in oil phase for oil film over hydration water layer on silica substrate.

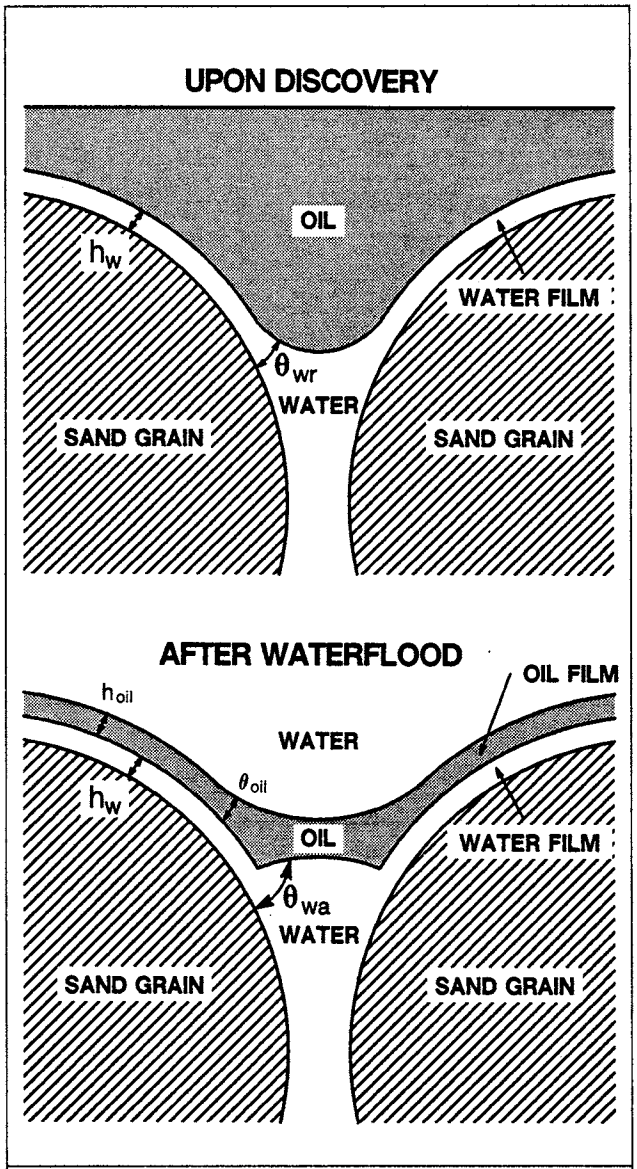

Fig. 15—Thin films and contact angles in rock pore space.

disjoining pressure is attractive, and the oil film would thin to nothing if nothing (e.g., an adsorbed asphaltene layer) existed to limit the thinning. At intermediate water-film thicknesses, the disjoining pressure changes sign with oil-film thickness. Eq. 7 shows that the interaction potential can change sign as a function of the oil-film thickness. **Fig. 14** shows the contact angle in the oil phase, if the oil-film thickness is limited by steric-type structural forces. If no adsorbed water layer exists, the contact angle (in the oil phase) is zero regardless of the limiting oil-film thickness; i.e., the oil is wetting the dehydrated quartz surface. In the absence of an adsorbed water layer, adsorption of surfactants in the oil and steric effects are not needed for oil wetting; i.e., the van der Waals interactions are sufficient. With increasing thickness of the adsorbed water layer, the limiting thickness of the oil film must also increase for the contact angle to be zero. If the limiting oil-film thickness is less than the diameter of an alkane chain (the continuum assumption breaks down for submonolayers) of 0.4 nm, the contact angle is very dependent on the value of the limiting thickness. If the oil-film thickness is limited by adsorption of asphaltene aggregates of about 1.0 nm diameter, then the contact angle is equal to or close to zero even with a thick adsorbed water layer. These results show that the contact angle in the oil phase is a function of the thickness of the adsorbed hydration water and the limiting cutoff thickness of the oil film, in addition to the van der Waals interactions.

This model of oil wetting and hysteresis resulting from a surfactant-stabilized film is consistent with the experimental observations of Aronson *et al.*[32] and Brown and Neustadter.[33] In Ref. 32, the oil-soluble surfactant *N,N*-dimethyldocosylamine spread spontaneously on the silica surface.

McGuiggan and Pashley[35] studied the effects of surfactants on contact angle hysteresis using air/aqueous surfactant solution/mica. The surfactant was dihexadecyldimethylammonium acetate, a surfactant with extremely low monomer solubility, forming bilayer aggregates in solution, and which adsorbs onto mica as either a monolayer or bilayer, depending on solution concentration. The initial water-advancing contact angle on a dry surface was about 90°. The static advancing contact angle slowly changed to somewhat less than the initial advancing contact angle. The initial receding angle, measured immediately after the contact line was advanced, was also only somewhat less than the initial advancing contact angle. If the system was allowed to equilibrate 0.5 to 3 hours, however, then the water-receding contact angle decreased to below 10°. These results demonstrate that significant time-dependent hysteresis effects take place when the surfactant is very large and has a very slow diffusion rate.

Films and Contact Angles in Pore Space

Two types of films and contact angles (illustrated in **Fig. 15**) have been discussed: water film with a contact angle in the water phase

and an oil film with a contact angle in the oil phase. The water film with the contact angle in the water phase could describe the fluid distribution as the oil initially enters the pore space. The oil film and the contact angle in the oil phase could describe the fluid distribution after a waterflood. Also, after the waterflood, the contact angle in the water phase could change as a result of movement of the contact line. The interrelationship of these contact angles with the pore geometry is needed to describe the effect of wettability on the capillary pressure and relative permeability curves and the residual oil saturation.

Recent Results and Needed Research

van der Waals Interactions. I have determined the van der Waals interactions, including the Hamaker constant, for combinations of 43 different materials using the complete Lifshitz theory[16,36] with the computer program provided by Gee.[37] The approximate formula (Eq. 4) is accurate at small thickness for quartz/water/alkane systems. It overestimates the exact (Lifshitz) value for aromatics. Retardation effects should be included for films thicker than 5 nm. The appropriate refractive index in the approximate formula is the value extrapolated to zero frequency, not the usual tabulated value at the Na D line. Our best estimate of the Hamaker constant for quartz/water/hexadecane is 0.85×10^{-20} J.

Electrostatic Interactions. Recent results by Buckley and Morrow[38] show that the wetting transition at low salinities corresponds to that predicted from the electrostatic and van der Waals calculations. However, high salinities indicate the importance of other mechanisms.

My experience has shown that extreme care must be taken to prepare and equilibrate samples for zeta potential measurements to have reproducible and correlatable results. Also, the ASTM D664-81[39] procedure cannot be used to measure the base content of crude oils.

Zeta potential measurements are needed for minerals other than glass and quartz. In addition to the pH, such minerals as calcite have zeta potentials that are a function of the calcium and carbonate concentrations.[40] The carbonate concentration is a function of the CO_2 partial pressure.

Traditional models of electrostatic interactions use the mean field approximation; e.g., surface charges are uniformly distributed and the ions are point charges. The thin films that exist in the case of finite contact angles may require consideration of such structural interactions as correlation of surface charges and specific ion effects. Models are needed for the charge regulation that must occur as two surfaces approach each other.

Structural and Solvation Interactions. Short-range structural and solvation interactions[41,42] are needed to explain the magnitude of the contact angle when it is nonzero. We have found that the interactions resulting from the discreteness of the fluid in a submonolayer can be modeled with a 2D equation of state to predict the contact angles and spreading coefficients of van der Waals fluids (no electrostatic or hydrogen-bonding interactions).[8] This establishes, in principle, that the contact angle can be predicted when the structural interactions are known.

The structural interaction information needed for petroleum reservoirs is the magnitude of the hydrogen-bonding (Lewis acid/base)[43,44] interaction of water and polar crude oil functional groups with mineral surfaces. Some results have been reported for silica and alumina surfaces using heat of adsorption, heat of immersion, temperature-programmed desorption, and infrared spectroscopy. Studies on minerals of interest to petroleum reservoirs are needed.

Force measurements of crude oil between two mica surfaces show that a thick, irreversibly adsorbed layer sometimes forms with time.[45] The thickness of this adsorbed oil layer is a parameter in the model for the water-advancing contact angle.

Rock Morphology. The rock morphology is beyond the scope of this paper. An understanding of the interactions between contact angle and rock morphology, however, is needed to provide a practical understanding for the practicing engineer.

Conclusions

1. The Hamaker constant for van der Waals interactions can be calculated from the dielectric constant, refractive index, and adsorption frequency of the materials.
2. The interaction of the electrical double layers on two surfaces as they approach each other results in interaction potentials that are either positive (repulsive), negative (attractive), or a combination.
3. The electrostatic interaction potential is a function of the magnitude and sign of the electrical potentials of the surfaces in isolation and of how the charge and potential change as the surfaces interact with each other.
4. The condition for the (meta)stability of a thick, wetting-water film on a flat surface with zero capillary pressure can be estimated from the electrical surface potentials in isolation, the Hamaker constant, and the electrolyte composition.
5. A thick, wetting-water film can be collapsed with increased capillary pressure and/or curvature (convex) of the solid substrate.
6. The contact angle with a thin water film is a function of the Hamaker constant and strongly depends on the limiting thickness of the hydration water.
7. The contact angle is also a function of the electrical potentials of the two surfaces, but the electrostatic interactions (assuming smeared charges) become less significant at high electrolyte concentrations. The thickness of the hydration water, however, may still depend on the mineral-surface charge and on the effect of discrete charges. The adsorption of an oil film still depends on the interface charges.
8. When advancing water moves the contact line, natural surfactants in the crude oil may retain an oil film on the substrate. In this case, the contact angle in the oil phase depends on the limiting thickness of both the hydration water and the oil film, in addition to the Hamaker constants.

Nomenclature

A = Hamaker constant, J
C = concentration, molecules/m^3
e = charge per electron, 1.602×10^{-19} C
F_{Φ_e} = ratio of electrical potentials
h = film thickness, m
h' = variable of integration, m
h_o = equilibrium film thickness
H = mean curvature, m^{-1}
k = Boltzmann's constant, 1.381×10^{-23} J/K
n = refractive index
p = pressure, Pa
P = Planck's constant, 6.626×10^{-34} J·s
P_c = capillary pressure, Pa
$S_{\gamma/\alpha\beta}$ = equilibrium spreading coefficient, J/m^2
T = temperature, K
z = valence of ion
α = local inclination angle of interface
δ = thickness of absorbed layer, m
Δ = $1-\cos\theta$
ϵ = relative permittivity or zero-frequency dielectric constant
ϵ_i = zero-frequency dielectric constant of Material i
ϵ_o = permittivity of free space, 8.854×10^{-12} C^2/J·m
θ = contact angle
κ = reciprocal Debye length, m^{-1}
μ_c = chemical potential, J/mol
ν_e = electronic absorption frequency, Hz
Π = disjoining pressure, Pa
σ = IFT, J/m^2
σ^f = film tension, J/m^2
Φ_e = electrical potential, V
Φ_g = gravitational potential, J/kg
ω = specific interaction potential, J/m^2
$\Delta\omega$ = departure from equilibrium ω, J/m^2
Ω = grand canonical potential, J

Author

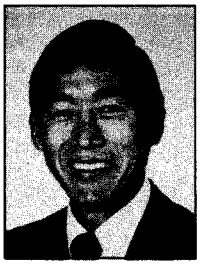

George J. Hirasaki is a research adviser in the Reservoir Mechanism Research Dept. of Shell Development Co. in Houston. He joined Shell in 1967 and worked for 2 years in the West Coast Div. as section leader of reservoir engineering. He holds a BS degree from Lamar U. and a PhD degree from Rice U., both in chemical engineering. Recipient of the 1989 Lester C. Uren award and editor of the SPE monograph *Reservoir Simulation*, Hirasaki served on program committees for the 1974 and 1976 Annual Meetings, on the 1981 Forum Series Committee, and on the Monograph Committee in 1975 and from 1982 to 1987.

Subscripts

a = advancing
D = dimensionless
eq = equilibrium
r = receding
w = water
α,β = bulk phases
γ = film phase
$\nu=0$ = zero frequency
$\nu>0$ = nonzero frequency
1,2,3 = materials or surfaces

References

1. Anderson, W.G.: "Wettability Literature Survey—Part 4: Effects of Wettability on Capillary Pressure," *JPT* (Oct. 1987) 1283–1300.
2. Anderson, W.G.: "Wettability Literature Survey—Part 5: The Effects of Wettability on Relative Permeability," *JPT* (Nov. 1987) 1453–68.
3. Israelachvili, J.N.: *Intermolecular and Surface Forces*, Academic Press, New York City (1985).
4. Derjaguin, B.V., Churaev, N.V., and Muller, V.M.: *Surface Forces*, Consultants Bureau, New York City (1987).
5. Derjaguin, B.V.: *Theory of Stability of Colloids and Thin Films*, Consultants Bureau, New York City (1989).
6. Derjaguin, B.V. and Churaev, N.V.: "Properties of Water Layers Adjacent to Interfaces," *Fluid Interfacial Phenomena*, C.A. Croxton (ed.), John Wiley & Sons, New York City (1986) Chap. 15.
7. Mohanty, K.K.: "Fluids in Porous Media: Two-Phase Distribution and Flow," PhD dissertation, U. of Minnesota, Minneapolis (1981).
8. *Interfacial Phenomena in Oil Recovery*, N.R. Morrow (ed.), Marcel Dekker Inc., New York City (1990) Chaps. 2 and 3.
9. Melrose, J.C.: "Interpretation of Mixed Wettability States in Reservoir Rocks," paper SPE 10971 presented at the 1982 SPE Annual Technical Conference and Exhibition, New Orleans, Sept. 26–29.
10. Hall, A.C., Collins, S.H., and Melrose, J.C.: "Stability of Aqueous Wetting Films in Athabasca Tar Sands," *SPEJ* (April 1983) 249–58.
11. Takamura, K.: "Microscopic Structure of Athabasca Oil Sand," *Cdn. J. Chem. Eng.* (Aug. 1982) **60**, 538–45.
12. Buckley, J.S., Takamura, K., and Morrow, N.R.: "Influence of Electrical Surface Charges on the Wetting Properties of Crude Oil," *SPERE* (Aug. 1989) 332–40.
13. Derjaguin, B.V.: *Zh. Fiz. Khim.* (1940) **14**, 137.
14. Derjaguin, B.V.: "Definition of the Concept of and Magnitude of the Disjoining Pressure and Its Role in the Statics and Kinetics of Thin Layers of Liquids," *Colloid J.* (1955) **17**, No. 3, 191–97.
15. Fumkin, A.N.: "Wetting and Adherence of Bubbles," *Zh. Fiz. Khim.* (1938) **12**, 337–45.
16. Hough, D.B. and White, L.R.: "The Calculation of Hamaker Constants from Lifshitz Theory with Application to Wetting Phenomena," *Adv. Colloid Interface Sci.* (1980) **14**, 3–41.
17. Bargeman, D. and Van Voorst Vader, F.: "van der Waals Forces Between Immersed Particles," *J. Electroanal. Chem.* (1972) **37**, 45–52.
18. Usui, S.: "Heterocoagulation," *Prog. Surface Membrane Sci.* (1972) **5**, 223–66.
19. Richmond, P.: "The Theory and Calculation of van der Waals Forces," *J. Colloid Sci.* (1975) **2**, 130–71.
20. Parsegian, V.A. and Ninham, B.W.: "Toward the Correct Calculation of van der Waals Interactions Between Lyophobic Colloids in an Aqueous Medium," *J. Colloid Interface Sci.* (1971) **37**, No. 2, 332–41.
21. Vold, M.J.: "The Effect of Adsorption on the van der Waals Interaction of Spherical Colloidal Particles," *J. Colloid Sci.* (1961) **16**, 1–12.
22. Vincent, B.: "The van der Waals Attraction Between Colloid Particles Having Adsorbed Layers. II. Calculation of Interaction Curves," *J. Colloid Interface Sci.* (1973) **42**, No. 2, 270–85.
23. Hogg, R., Healy, T.W., and Fuerstenau, D.W.: "Mutual Coagulation of Colloidal Dispersions," *Trans.*, Faraday Soc. (1966) **62**, 1638–51.
24. Usui, S.: "Interaction of Electrical Double Layers at Constant Surface Charge," *J. Colloid Interface Sci.* (1973) **44**, No. 1, 107–13.
25. Chan, D., Healy, T.W., and White, L.R.: "Electrical Double Layer Interactions under Regulation by Surface Ionization Equilibria—Dissimilar Amphoteric Surfaces," *J. Chem. Soc. Faraday Trans. I* (1976) **72**, 2844–65.
26. Hunter, R.J.: "Zeta Potential in Colloid Science," *Principles and Applications*, Academic Press, Washington, DC (1981).
27. Fuerstenau, D.W.: "Interfacial Processes in Mineral/Water Systems," *Pure Applied Chem.* (1970) **24**, 135–64.
28. James, R.O. and Parks, G.A.: "Characterization of Aqueous Colloids by Their Electrical Double-Layer and Intrinsic Surface Chemical Properties," *Surface and Colloid Science*, E. Matijevic (ed.), Plenum Press, New York City (1982) **12**, 119–216.
29. Somasundaran, P. and Agar, G.E.: "The Zero Point of Charge of Calcite," *J. Colloid Interface Sci.* (1967) **24**, 433–40.
30. van Olphen, H.: *An Introduction to Clay Colloid Chemistry*, second edition, John Wiley & Sons, New York City (1977).
31. Israelachvili, J.: "Solvation Forces and Liquid Structure as Probed by Direct Force Measurements," *Accounts Chem. Res.* (1987) **20**, 415–21.
32. Aronson, M.P., Petko, M.F., and Princen, H.M.: "On the Stability of Aqueous Films Between Oil and Silica," *J. Colloid Interface Sci.* (June 1978) **65**, No. 2, 296–306.
33. Brown, C.E. and Neustadter, E.L.: "The Wettability of Oil/Water/Silica Systems with Reference to Oil Recovery," *J. Cdn. Pet. Tech.* (July–Sept. 1980) 100–10.
34. Christensen, H.K. and Israelachvili, J.N.: "Direct Measurements of Interactions and Viscosity of Crude Oils in Thin Films Between Model Clay Surfaces," *J. Colloid Interface Sci.* (Sept. 1987) **119**, No. 1, 194–202.
35. McGuiggan, P.M. and Pashley, R.M.: "A Study of Surfactant Solution Wetting on Mica," *Colloids and Surfaces* (1987) **27**, 277–87.
36. Dzyaloshinskii, I.E., Lifshitz, E.M., and Pitaevskii, L.P.: "The General Theory of van der Waals Forces," *Advan. Phys.*, **10**, 165–209.
37. Gee, M.L.: "Surface Forces in Thin Liquid Films on Quartz," PhD dissertation, U. Melbourne, Melbourne, Australia (1987).
38. Buckley, J.S. and Morrow, N.R.: "Characterization of Crude Oil Wetting Behavior by Adhesion Tests," paper SPE 20263 presented at the 1990 SPE/DOE Symposium on Enhanced Oil Recovery, Tulsa, April 22–25.
39. "ASTM D664-81, Standard Test Methods for Neutralization Number by Potentiometric Titration," *Annual Book of ASTM Standards*, Am. Soc. Testing Materials, Philadelphia (1983) **05.01**, Sect. 5, 327.
40. Thompson, D.W. and Pownall, P.G.: "Surface Electrical Properties of Calcite," *J. Colloid Interface Sci.* (1989) **131**, No. 1, 74–82.
41. Christenson, H.K.: "Non-DLVO Forces Between Surfaces—Solvation, Hydration, and Capillary Effects," *J. Disp. Sci. Tech.* (1988) **9**, No. 2, 171–206.
42. Derjaguin, B.V. and Churaev, N.V.: "The Current State of the Theory of Long-Range Surface Forces," *Colloids and Surfaces* (1989) **41**, 223–37.
43. van Oss, C.J., Chaudhury, M.K., and Good, R.J.: "Interfacial Lifshitz-van der Waals and Polar Interactions in Macroscopic Systems," *Chem. Rev.* (1988) **88**, 927–41.
44. Costanzo, P.M., Giese, R.F., and van Oss, C.J.: "Determination of the Acid-Base Characteristics of Clay Mineral Surfaces by Contact Angle Measurements—Implications for the Adsorption of Organic Solutes from Aqueous Media," *J. Adhesion Sci. Tech.* (1990) **4**, No. 4, 267–75.
45. Fang, J. and Christenson, H.K.: "Viscosity and Adsorption Studies of Australian Crude Oils in Thin Films," *J. Disp. Sci. Tech.* (1990) **11**, No. 2, 97–114.

SI Metric Conversion Factors

Å	× 1.0*	E−01	=	nm
Btu	× 1.055 056	E+00	=	kJ
dynes/cm	× 1.0*	E+00	=	mN/m
ft²	× 9.290 304*	E−02	=	m²
°F	(°F−32)/1.8		=	°C
psi	× 6.894 757	E+00	=	kPa

*Conversion factor is exact.

SPEFE

Original SPE manuscript received for review March 18, 1988. Paper accepted for publication Jan. 11, 1991. Revised manuscript received Nov. 28, 1990. Paper (SPE 17367) first presented at the 1988 SPE/DOE Enhanced Oil Recovery Symposium held in Tulsa, April 17–20.